

Sound velocities of hexagonal close-packed H₂ and He under pressure

Yu. A. Freiman,^{1,*} Alexei Grechnev,¹ S. M. Tretyak,¹ A. F. Goncharov,² C. S. Zha,² and Russell J. Hemley²

¹*B. Verkin Institute for Low Temperature Physics and Engineering of the National Academy of Sciences of Ukraine, 47 Lenin avenue, Kharkov, 61103, Ukraine*

²*Geophysical Laboratory, Carnegie Institution of Washington, 5251 Broad Branch Road NW, Washington, DC 20015, USA*

Bulk, shear, and compressional aggregate sound velocities of hydrogen and helium in the close-packed hexagonal structure are calculated over a wide pressure range using two complementary approaches: semi-empirical lattice dynamics based on the many-body intermolecular potentials and density-functional theory in the generalized gradient approximation. The sound velocities are used to calculate pressure dependence of the Debye temperature. The comparison between experiment and first-principle and semi-empirical calculations provide constraints on the density dependence of intermolecular interactions in the zero-temperature limit.

PACS numbers: 67.80.F-,67.80.B-,62.20.dj

Hydrogen and helium are the simplest and most abundant chemical elements in the Universe. Studies of solid helium and hydrogen at elevated pressures, which started at the end of the 1920s, are of great interest for many branches of science. Hydrogen and helium are major constituents of stars and giant planets and their physical properties are very important for condensed matter physics, planetary science and astrophysics. As such the behavior of these elements under extreme environments of pressure and temperature is central to modeling the interiors of planetary and astrophysical bodies.

High-pressure x-ray, Raman and infra-red (IR) studies established three molecular phases of solid hydrogen¹⁻⁴. These phases are related to the orientational ordering of the molecules and structural transitions. In phase I, which is stable at zero temperature up to 110 GPa, hydrogen molecules are quantum rotors arranged in the hexagonal-close-packed (hcp) structure. At the I - II phase transition the molecules go from the quantum rotor state to a strongly anharmonic anisotropic librational state. Above 150 GPa solid hydrogen transforms to phase III. The molecular ordering in this phase can be treated classically. Thus, for this part of the phase diagram the most general picture can be formulated in terms of the concept of quantum versus classical orientational ordering⁵. Although the structures of phases II and III are unknown, x-ray and Raman data suggest that the hydrogen molecules in both phases lie close to the sites of the hcp lattice^{6,7}. At low temperatures the molecules are stable to at least 360 GPa; but hydrogen transforms to new phases (e.g., phase IV) with increasing temperature at these pressures⁸⁻¹¹.

At low pressures and temperatures ⁴He crystallizes into the hcp structure. High-pressure x-ray diffraction measurements¹²⁻¹⁴ have shown that in a wide temperature (up to 400 K) and pressure (up to 58 GPa) range hcp ⁴He is stable with the exception of two narrow segments adjacent to the melting curve (25.9 - 30.4 bar, bcc, and 0.1 - 11.6 GPa, fcc). The highest volume compression reached in the equation of state (EOS) experiments is $V_0/V = 10.4$ at 180 GPa for solid hydrogen⁶ ($V_0/V = 7.6$

for solid D₂¹⁵), and $V_0/V = 8.4$ for solid helium¹³.

The phonon spectra of hcp hydrogen and helium exhibits a Raman-active optical mode of the E_{2g} symmetry. The frequency $\nu(P)$ of this mode calculated with various semi-empirical (SE) potentials is highly sensitive to details of the calculation scheme, making it a stringent test for any potential or theoretical method, e.g., density functional theory (DFT). The frequency range of this mode in solid hydrogen as a function of pressure is extremely large: from 36 cm⁻¹ at zero pressure¹⁶ to 1100 cm⁻¹ at 250 GPa^{17,18}. For solid helium the situation is different: neutron measurements performed close to the solidification pressure¹⁹ gave about 50 cm⁻¹ for the E_{2g} -mode frequency; Raman measurements under pressure of about 1 GPa²⁰ gave frequency about 74 cm⁻¹. Higher pressure measurements have not revealed any Raman activity^{21,22}. According to DFT and semi-empirical (SE) calculations²³ at the highest reached compressions the Raman frequency is about 500 cm⁻¹.

Sound velocity is another experimentally measurable quantity which provides information on the elastic moduli, elastic anisotropy, equation of state, and other thermodynamic properties. At low pressures, the lattice dynamics of solid hydrogen and helium is governed by strongly anharmonic and quantum crystal effects. The use of the self-consistent phonon (SCP) approach made it possible to reach good agreement between theoretical²⁴⁻²⁶ and measured sound velocities and elastic moduli²⁷⁻²⁹ for parahydrogen and orthodeuterium. The situation is similar for solid helium: there is a good correspondence between early experimental results³⁰⁻³² and SCP theories³³⁻³⁵. A detailed review of early literature for solid helium was given by Trickey *et al.*³⁶.

The problem of supersolid have rekindled interest in experimental^{37,38} and theoretical³⁹⁻⁴² studies of elastic properties of solid helium in the quantum crystal region. At the same time, studies of elastic properties of solid hydrogen and solid helium at elevated pressures are rather scarce. Liebenberg *et al.*⁴³ measured the sound velocities in solid hydrogen from 0.4 to 1.9 GPa using the piston-cylinder technique. Zha *et al.*⁴⁴ and Duffy *et al.*⁴⁵ studied

the elasticity of solid hydrogen in the pressure range up to 24 GPa by single-crystal Brillouin scattering. In solid helium the aggregate quasi-compressional sound velocity v_P to 20 GPa was found by combing results of two experiments: Polian and Grimsditch²² measured the product of v_P and the refractive index n by using Brillouin scattering in the backscattering geometry, and Le Toullec *et al.* made a separate refractive-index measurements⁴⁶. The direct data on the sound velocities in solid helium up to 32 GPa were obtained by the single-crystal Brillouin scattering measurements by Zha *et al.*¹⁴.

The goal of the present paper is to calculate the pressure dependence of sound velocities of hcp H₂ and He over a wide range of pressures and compare with existing experimental data. No explicit effects of electronic excitations or changes in molecular bonding (e.g., as a function of temperature) are assumed. As such, the results provide a baseline for comparison with more elaborate models (e.g., that go beyond DFT or include thermal effects). The calculations were carried out using the DFT and semi-empirical (SE) approaches. The results for hydrogen extend our previous results⁴⁷. The elastic properties of He under pressure were previously investigated within DFT using an atomic-based EMTO code⁴⁸. Unfortunately, the small-scale figures shown in Ref. 48 render a quantitative comparison, in particular, with the SE results difficult. The comparison of the SE and DFT-GGA results shows that these two approaches complement each other⁷: at lower pressures SE gives more accurate results but with increasing pressure DFT-GGA becomes preferable.

The hydrodynamic or bulk sound velocity v_B was found from the EOS:

$$v_B = [\partial P / \partial \rho]^{1/2} = \left[-\frac{V^2}{\mu} \frac{\partial P}{\partial V} \right]^{1/2}, \quad (1)$$

where P is the pressure, ρ is the density, μ is the molar mass, and V is the molar volume.

The shear velocity v_S was obtained from the the shear elastic constant C_{44} , which was in turn calculated from the Raman frequency $\nu(E_{2g})$ using the relation⁴⁹:

$$\nu(E_{2g}) = \left(4\sqrt{3}a^2 C_{44} / (mc) \right)^{1/2}, \quad (2)$$

where a , c are the lattice parameters and m is the molecular mass. This relation was used in Ref. 49 for solid He under pressure.

In the framework of the Voigt-Reuss-Hill averaging scheme⁵⁰⁻⁵⁴ the relation between the isotropically averaged aggregate compressional, v_P , bulk, v_B , and shear, v_S , sound velocities holds⁵⁵

$$v_P^2 = v_B^2 + \frac{4}{3}v_S^2. \quad (3)$$

Using this equation we calculated the aggregate compressional sound velocity v_P which together with v_B and v_S

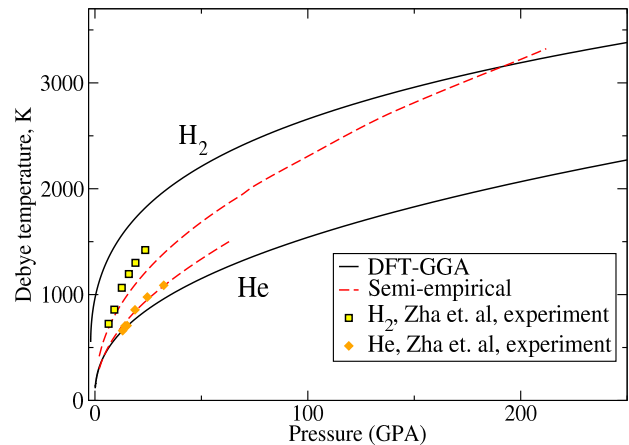


FIG. 1: (Color online) Debye temperature in solid H₂ and He as a function of pressure. Theoretical many-body SE and DFT-GGA results (this work), and experimental data for H₂⁴⁴ and He¹⁴ are presented.

made it possible to calculate the Debye temperature Θ_D :

$$\Theta_D = \frac{\hbar}{k_B} \left[\frac{V}{18\pi^2 N_A} \left(\frac{1}{v_P^3} + \frac{2}{v_S^3} \right) \right]^{-1/3}, \quad (4)$$

where k_B is the Boltzmann constant and N_A is the Avogadro number.

We start with the DFT calculations. The sound velocities v_B , v_S in H₂ and He were calculated within DFT using the generalized gradient approximation (GGA)⁵⁶. All calculations were done using the full-potential linear muffin-tin orbital (FP-LMTO) code RSPt⁵⁷ for zero temperature. The $Pca2_1$ structure was used for hydrogen. The zero-point vibrations (ZPV) of the nuclei were ignored in the initial calculations.

The bulk sound velocities were calculated from the parametrized DFT EOS $P(V)$ by numerical differentiation (Eq. (1)). The shear sound velocities were found from the DFT Raman frequencies (Eq. (2)), which were in turn obtained from supercell total energy calculations and parametrized to allow for a smooth numerical differentiation of the Debye temperature. 693 and 1331 k -points in the Brillouin zone were used for H₂ and He, respectively, and the convergence of the results with the number of k -points was checked. GGA EOS was used to obtain P -dependent sound velocities from the V -dependent ones. As a result, from Eqs. (1) - (3) we obtained the zero-order aggregate sound velocities and from Eq. (4) we obtained the Debye temperature Θ_D (Fig. 1).

The ZPV were taken into account in our DFT-GGA approach within the framework of the Debye model. The ZPV correction to the EOS is

$$\Delta P(V) = -\frac{9}{8} N_A k_B \frac{d\Theta_D}{dV}, \quad (5)$$

This formula was used to calculate the ZPV-corrected $P(V)$ and $v_B(V)$ from the original (non-ZPV-corrected)

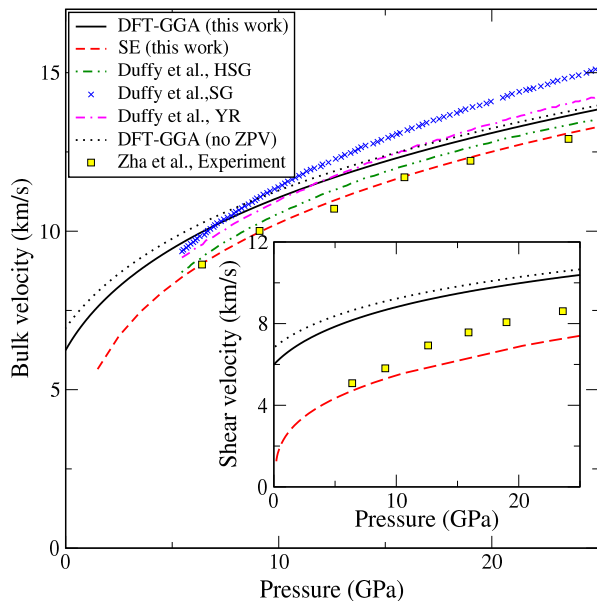


FIG. 2: (Color online) Bulk sound velocity in solid H_2 as a function of pressure. Theoretical results obtained using many-body SE and DFT-GGA including and disregarding ZPV (this work), SE with pair potentials SG⁴⁵, HSG⁴⁵ and YR⁴⁵, and the experimental data⁴⁴ are presented. The inset shows the SE and DFT-GGA shear sound velocities (this work) in comparison with experiment⁴⁴.

$v_B(V)$, $v_S(V)$. The shear velocity $v_S(V)$ is not affected by ZPV in our approximation. Finally, the ZPV-corrected EOS is used to calculate the ZPV-corrected P -dependent velocities $v_B(P)$ and $v_S(P)$.

We now turn to the SE calculations. A variety of pair potentials have been tested in EOS and Raman studies of solid hydrogens^{45,58–60}. One of the first was the low-pressure Silvera - Goldman potential (SG)⁵⁸. The first DAC experiments found it to be too stiff, i.e. the repulsion increases too rapidly with pressure. Hemley *et al.*^{45,60} modified the SG potential⁵⁸ with a short-range correcting term. This Hemley-Silvera-Goldman effective potential (HSG) as well as other pair potentials, e.g. the Young-Ross (YR) potential⁵⁹, were shown to fit the experimental EOS well up to 40 GPa, but they are still too stiff at yet higher pressures¹⁵. A similar situation takes place for helium^{13,61}. The reason is the neglect of the three body and higher-order terms in the intermolecular potential^{7,23,61–65}. First-principles methods and SE approaches which take into account such terms work well up to the highest pressures reached in EOS and Raman measurements⁷.

The many-body hydrogen intermolecular potential used here is a sum of the pair SG potential⁵⁸ (discarding the R^{-9} term) and two three-body terms: the long-range Axilrod-Teller dispersive interaction and the short-range three-body exchange interaction in the Slater-Kirkwood form^{23,62}. The explicit form and parameters of the potential used in this work for solid hydrogen are given in

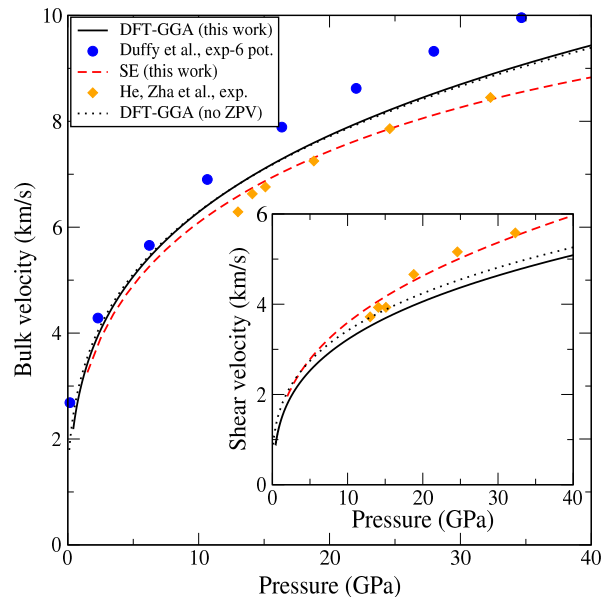


FIG. 3: (Color online) Bulk sound velocity in solid He as a function of pressure. Theoretical results obtained using many-body SE and DFT-GGA including and disregarding ZPV (this work), SE with exp - 6 pair potential⁴⁵, and the experimental data¹⁴ are presented. The inset shows the SE and DFT-GGA shear sound velocities (this work) in comparison with experimental results¹⁴.

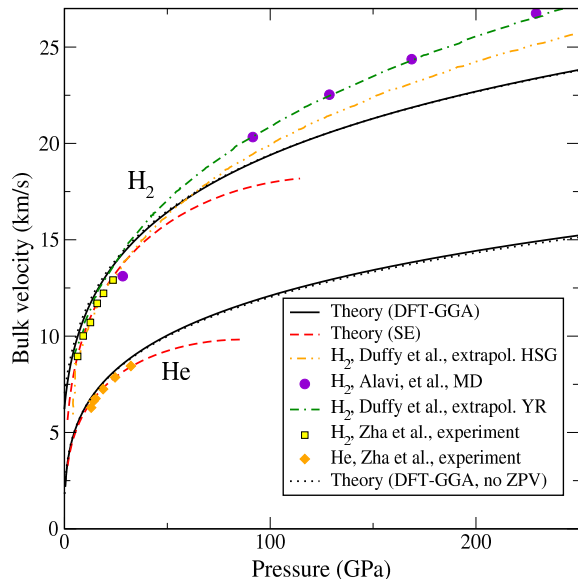


FIG. 4: (Color online) Bulk sound velocity in solid H_2 and He as a function of pressure for the extended pressure range. Theoretical many-body SE and DFT-GGA results including and disregarding ZPV (this work), first-principle MD results⁶⁸, SE with HSG and exp - 6 pair potentials⁴⁵, and experimental data^{14,44} are presented.

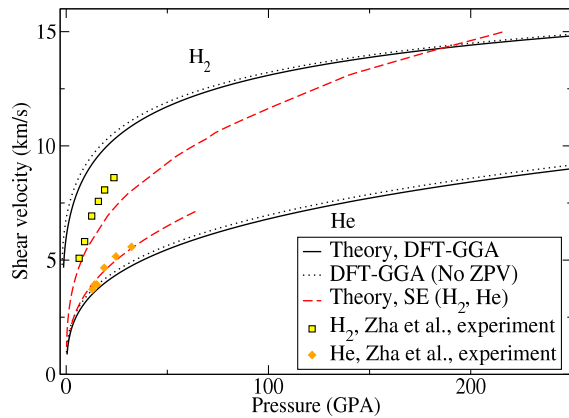


FIG. 5: (Color online) Shear sound velocities of hcp hydrogen and helium for the extended pressure range. Theoretical many-body SE and DFT-GGA results including and disregarding zero-point vibrations (ZPV) (this work), and experimental data^{14,44} are presented.

Ref. 63. The interatomic potential for solid helium has a similar form^{23,61,62}. For the two-body interaction, we used the HFDHE2 Aziz *et al.* potential⁶⁶. We also tested the HFD-B3-FCI1 Aziz potential⁶⁷ and found that the results for these two pair potentials practically coincide. The explicit form of the potential used for solid helium are given in Ref. 61. In our calculations we restrict ourselves to $T = 0$ K, with the zero-point energy treated in the Einstein approximation.

The calculated bulk and shear sound velocities for H_2 and He are shown in Figs. (2) and (3) for solid H_2 and He, respectively. The many-body SE bulk velocities are in excellent agreement with the data from Brillouin scattering measurements^{14,44,45}. Since the empirical SG¹⁶ and HSG⁶⁰ potentials for H_2 tend to overestimate the repulsive part of the intermolecular interaction, they also underestimate the compressibility and overestimate the sound velocity. Thus, the stiffer the potential is, the greater the error. The same conclusion follows from the comparison of the bulk sound velocity in solid He calculated from the many-body potential and far more rigid exp-6 potential (Fig. 3). As for DFT-GGA results, in the pressure range shown in Figs. 2 and 3 their accuracy are markedly below that of the SE results which reflects

the fact that DFT-GGA does not treat the van der Waals interaction properly.

In order to make a proper comparison of the results of the both approaches we calculated the sound velocities over a broad range of pressures in the ideal hcp structure. Figures (4) and (5) present the bulk and shear sound velocities, respectively, in solid H_2 and He calculated with our SE and DFT-GGA methods for the extended pressure range up to 250 GPa. The first-principles molecular dynamics (MD) results⁶⁸ for H_2 by Alavi *et al.*, and the SE results by Ross *et al.*⁵⁹ (HSG and YR potentials) extrapolated by Duffy *et al.*⁴⁵, are also presented for comparison. Although the MD results by Alavi *et al.* agree well with the extrapolated YR results, they are still significantly higher than our SE and DFT-GGA results.

A rather narrow range of pressures where experimental results^{14,44} exist did not permit unambiguous bounds on the applicability of the DFT-GGA and SE approaches used in the sound velocity calculations. Judging from Figs. (4) and (5), upper bounds for the SE approach are approximately 75 GPa and approximately 50 GPa for H_2 and He, respectively, and the lower bound for the DFT-GGA is around 100 GPa both for H_2 and He. So the upper bound for the SE and the lower bound for the DFT-GGA do not overlap and there is an intermediate pressure range where both methods are ineffective. It should be noted that the ranges of applicability of the SE approach are different for the EOS⁷, Raman⁷, and sound velocity calculations.

In conclusion, the bulk and shear sound velocities in solid H_2 and He calculated with the SE many-body intermolecular potential are in good agreement with experiment. At low pressures the accuracy of the SE approach is much higher than that of the DFT-GGA, but for pressures over 100 GPa the latter approach is preferable. The results can serve as a baseline for planetary and astrophysical models and provide a basis for extrapolation to more extreme conditions.

The work was supported by the National Nuclear Security Administration, Centre for Development of Advanced Computing, and NSF DMR 1106132. A.F.G. acknowledges support from the NSF, Army Research Office, NASA Astrobiology Institution, and Energy Frontier Research in Extreme Environments.

* Electronic address: freiman@ilt.kharkov.ua

¹ I. F. Silvera, Rev. Mod. Phys. **52**, 393 (1980).

² H.-k. Mao and R. J. Hemley, Rev. Mod. Phys. **66**, 671 (1994).

³ *Physics of Cryocrystals*, eds. V. G. Manzhelii and Yu. A. Freiman (AIP Press, New York, 1997).

⁴ J. Van Kranendonk: *Solid Hydrogen* (Plenum, N.Y., 1983).

⁵ I. I. Mazin, R. J. Hemley, A. F. Goncharov, M. Hanfland, and H.-k. Mao, Phys. Rev. Lett. **78**, 1066 (1997).

⁶ Y. Akahama, M. Nishimura, H. Kawamura, N. Hirao, Y.

Ohishi, and K. Takemura, Phys. Rev. B **82**, 060101(R) (2010).

⁷ Yu. A. Freiman, A. Grechnev, S. M. Tretyak, A. F. Goncharov, and R. J. Hemley, Phys. Rev. B **86**, 014111 (2012).

⁸ M. I. Eremets, I. A. Troyan, Nat. Mater. **10**, 927 (2011).

⁹ R. T. Howie, C. L. Guillaume, T. Scheler, A. F. Goncharov, and E. Gregoryanz, Phys. Rev. Lett. **108**, 125501 (2012).

¹⁰ C. S. Zha, Z. Liu, and R. J. Hemley, Phys. Rev. Lett. **108**, 146402 (2012).

¹¹ C. S. Zha, Z. Liu, M. Ahart, R. Boehler, and Russell J.

- Hemley, Phys. Rev. Lett. **110**, 217402 (2013).
- ¹² H.-k. Mao, R. J. Hemley, Y. Wu, *et al.*, Phys. Rev. Lett **60**, 2649 (1988).
- ¹³ P. Loubeyre, R. LeToullec, J. P. Pinceaux, H.-k. Mao, J. Hu, and R. J. Hemley, Phys. Rev. Lett **71**, 2272 (1993).
- ¹⁴ C. S. Zha, H.-k. Mao, and R. J. Hemley, Phys. Rev. B **70**, 174107 (2004).
- ¹⁵ P. Loubeyre, R. Le Toullec, D. Hausermann, M. Hanfland, R. J. Hemley, H.-k. Mao, and L. W. Finger, Nature **383**, 702 (1996).
- ¹⁶ I. F. Silvera, W. N. Hardy, and J. P. McTague, Phys. Rev. B **5**, 1578 (1972).
- ¹⁷ A. F. Goncharov, R. J. Hemley, H.-k. Mao, and J. Shu, Phys. Rev. Lett. **80**, 101 (1998).
- ¹⁸ A. F. Goncharov, E. Gregoryanz, R. J. Hemley, and H.-k. Mao, PNAS **98**, 14234 (2001)
- ¹⁹ J. Eckert, W. Thomlinson, and G. Shirane, Phys. Rev. B **16**, 1057 (1977); **18**, 3074 (1978).
- ²⁰ G. H. Watson and W. B. Daniels, Phys. Rev. B **31**, 4705 (1985).
- ²¹ A. F. Goncharov, unpublished.
- ²² A. Polian and M. Grimsditch, Europhys. Lett. **2**, 849 (1986).
- ²³ Yu. A. Freiman, A. F. Goncharov, S. M. Tretyak, A. Grechnev, J. S. Tse, , D. Errandonea, H.-k. Mao, and R. J. Hemley, Phys. Rev. B **78**, 014301 (2008).
- ²⁴ V. V. Goldman, J. Low Temp. Phys. **36**, 521 (1979).
- ²⁵ V. V. Goldman, Phys. Rev. B **20**, 4478 (1979).
- ²⁶ V. V. Goldman, J. Low Temp. Phys. **38**, 149 (1980).
- ²⁷ R. Wanner and H. Meyer, J. Low Temp. Phys. **13**, 337 (1973).
- ²⁸ P. J. Thomas, S. C. Rand, and B. P. Stoicheff, Can. J. Phys. **56**, 149 (1978).
- ²⁹ M. Nielsen, Phys. Rev. B **7**, 1626 (1973).
- ³⁰ J. P. Frank and R. Wanner, Phys. Rev. Lett **25**, 345 (1970).
- ³¹ R. H. Crepeau, O. Heybey, D. M. Lee, and S. A. Strauss, Phys. Rev. A **3**, 1162 (1971).
- ³² D. S. Greywall, Phys. Rev. A **3**, 2106 (1971); Phys. Rev. B **16**, 5127 (1977).
- ³³ V. V. Goldman, G. K. Horton, and M. L. Klein, Phys. Rev. Lett. **24**, 1424 (1971).
- ³⁴ H. Horner, Solid St. Commun. **9**, 79 (1971).
- ³⁵ N. S. Gillis, T. R. Koehler, and N. R. Werthamer, Phys. Rev. **175**, 1110 (1968).
- ³⁶ S. Trickey, W. Kirk, E. Adams, Rev. Mod. Phys. **44**, 668 (1972).
- ³⁷ J. Day, and J. Beamish, Nature **450**, 853 (2007).
- ³⁸ O. Syshchenko, J. Day, and J. Beamish, J. Phys.: Condensed Matter **21**, 164204 (2009).
- ³⁹ C. Cazorla, and J. Boronat, J. Phys.: Condensed Matter **20**, 015223 (2008).
- ⁴⁰ C. Cazorla, Y. Lutsyshyn, and J. Boronat, Phys. Rev. B **85**, 024101 (2012).
- ⁴¹ C. Cazorla, Y. Lutsyshyn, and J. Boronat, Phys. Rev. B **87**, 214522 (2013).
- ⁴² R. Pessoa, S. A. Vitiello, and M. de Koning, Phys. Rev. Lett. **104**, 085301 (2010).
- ⁴³ D. H. Liebenberg, R. L. Mills, and J. C. Bronson, Phys. Rev. B **18**, 4526 (1978).
- ⁴⁴ C. S. Zha, T. S. Duffy, H.-k. Mao, and R. J. Hemley, Phys. Rev. B **48**, 9246 (1993).
- ⁴⁵ T. S. Duffy, W. Vos, C. S. Zha, R. J. Hemley, and H.-k. Mao, Science **263**, 1590 (1994).
- ⁴⁶ R. Le Toullec, P. Loubeyre, and J.-P. Pinceaux, Phys. Rev. B **40**, 2368 1989.
- ⁴⁷ Yu. A. Freiman, A. Grechnev, S. M. Tretyak, A. F. Goncharov, and R. J. Hemley, Low Temp. Phys. **39**, 423 (2013).
- ⁴⁸ Z. Nabi, L. Vitos, B. Johansson, and R. Ahuja, Phys. Rev. B **72**, 172102 (2005).
- ⁴⁹ H. Olijnyk and A. P. Jephcoat, J. Phys.: Condens. Matter **12**, 10423 (2000).
- ⁵⁰ W. Voigt, *Lehrbuch der Kristallphysik*, Teubner, Leipzig and Berlin, 1910.
- ⁵¹ A. Reuss, Z. Angew. Math. Mech. **9**, 55 (1929).
- ⁵² R. Hill, Proc. Phys. Soc. **A65**, 349 (1952).
- ⁵³ P. Korpiun and E. Lüsher, *Thermal and Elastic Properties at Low Pressure*, in: *Rare Gas Solids* edited by M. L. Klein and J. A. Venables (Academic Press, London, 1977), Vol. II, p. 743.
- ⁵⁴ G. Steinle-Neumann, L. Stixrude, and R. E. Cohen, Phys. Rev. B **60**, 791 (1999).
- ⁵⁵ L. Anderson, J. Phys. Chem Solids **24**, 909, 1963.
- ⁵⁶ J. P. Perdew, K. Burke, and M. Ernzerhof, Phys. Rev. Lett., **77**, 3865 (1996).
- ⁵⁷ J. M. Wills, M. Alouani, P. Andersson, A. Delin, O. Eriksson, and O. Grechnev, *Full-Potential Electronic Structure Method: Energy and Force Calculations with Density Functional and Dynamical Mean Field Theory*, Springer, Berlin, 2010.
- ⁵⁸ I. F. Silvera and V. V. Goldman, J. Chem. Phys. **69**, 4209 (1978).
- ⁵⁹ M. Ross, F. H. Ree, and D. A. Young, J. Chem. Phys. **79**, 1487 (1983).
- ⁶⁰ R. J. Hemley, H.-k. Mao, L. W. Finger, A. P. Jephcoat, R. M. Hazen, and C. S. Zha, Phys. Rev. B **42**, 6458 (1990).
- ⁶¹ Yu. A. Freiman and S. M. Tretyak, Low Temp. Phys. **33**, 545 (2007).
- ⁶² P. Loubeyre, Phys. Rev. Lett. **58**, 1857 (1987); Phys. Rev. B **37**, 5432 (1988).
- ⁶³ Yu. A. Freiman, S. M. Tretyak, A. F. Goncharov, H.-k. Mao, and R. J. Hemley, Low Temp. Phys. **37**, 1308 (2011).
- ⁶⁴ Yu. A. Freiman, S. M. Tretyak, A. Grechnev, A. F. Goncharov, J. S. Tse, D. Errandonea, H.-k. Mao, and R. J. Hemley, Phys. Rev. B **80**, 094112 (2009).
- ⁶⁵ A. Grechnev, S. M. Tretyak, and Yu. A. Freiman, Low Temp. Phys. **36**, 333 (2010).
- ⁶⁶ R. A. Aziz, V. P. S. Nain, J. S. Carley, W. L. Taylor, and G. T. McConville, J. Chem. Phys. **70**, 4330 (1979).
- ⁶⁷ R. A. Aziz, A. R. Janzen, M. R. Moldover, Phys. Rev. Lett **74**, 1586 (1995).
- ⁶⁸ A. Alavi, M. Parrinello, and D. Frenkel, Science **269**, 1252 (1995).